



## Multimodal tract-based analysis in ALS patients at 7T: A specific white matter profile?

Esther Verstraete, Daniel L. Polders, René C. W. Mandl, Martijn P. Van Den Heuvel, Jan H. Veldink, Peter Luijten, Leonard H. Van Den Berg & Johannes Hoogduin


**To cite this article:** Esther Verstraete, Daniel L. Polders, René C. W. Mandl, Martijn P. Van Den Heuvel, Jan H. Veldink, Peter Luijten, Leonard H. Van Den Berg & Johannes Hoogduin (2014) Multimodal tract-based analysis in ALS patients at 7T: A specific white matter profile?, Amyotrophic Lateral Sclerosis and Frontotemporal Degeneration, 15:1-2, 84-92


**To link to this article:** <http://dx.doi.org/10.3109/21678421.2013.844168>

 View supplementary material 

 Published online: 10 Dec 2013.

 Submit your article to this journal 

 Article views: 130

 View related articles 

 View Crossmark data 

ORIGINAL ARTICLE

## Multimodal tract-based analysis in ALS patients at 7T: A specific white matter profile?

ESTHER VERSTRAETE<sup>1\*</sup>, DANIEL L. POLDERS<sup>2\*</sup>, RENÉ C. W. MANDL<sup>3</sup>,  
MARTIJN P. VAN DEN HEUVEL<sup>3</sup>, JAN H. VELDINK<sup>1</sup>, PETER LUIJTEN<sup>2</sup>,  
LEONARD H. VAN DEN BERG<sup>1</sup> & JOHANNES HOOGDUIN<sup>2</sup>

*Departments of <sup>1</sup>Neurology and <sup>3</sup>Psychiatry, Rudolf Magnus Institute of Neuroscience, University Medical Centre Utrecht, and <sup>2</sup>Department of Radiology, University Medical Centre Utrecht, Utrecht, The Netherlands*

### Abstract

Our objective was to explore the value of additional MR contrasts in elucidating the decrease in fractional anisotropy (FA) as has been observed in the corticospinal tracts (CST) of patients with amyotrophic lateral sclerosis (ALS). Eleven patients and nine healthy control subjects were scanned at 3T and 7T MRI. Whole brain and tract specific comparison was performed of both diffusion weighted (3T), quantitative  $T_1$  ( $qT_1$ ), magnetization transfer ratio (MTR) and amide proton transfer weighted (APT<sub>w</sub>) imaging (7T). Results of whole brain comparison using histogram analyses showed no significant differences between patients and controls. Measures along the CST showed a significantly reduced FA together with a significantly increased diffusivity perpendicular to the tract direction in patients compared to controls. In addition, patients showed a small but significant increase in MTR values within the right CST. No significant changes were observed in  $qT_1$  and APT<sub>w</sub> values. In conclusion, our findings, based on a multimodal approach, revealed that the decrease in FA is most probably caused by an increased diffusivity perpendicular to the CST. This diffusivity profile, together with the increase in MTR is inconsistent with demyelination but consistent with an increase of free liquid spins in the white matter tissue.

**Key words:** *Amyotrophic lateral sclerosis, diffusion tensor imaging, DTI*

### Introduction

The upper motor neurons in the brain and the lower motor neurons in the brainstem or spinal cord are connected through the corticospinal tract (CST), the great white matter ‘highway’ of the motor system. This tract has consistently been found to show degenerative effects in patients with amyotrophic lateral sclerosis (ALS), both in post mortem and in imaging studies (1,2). Most notably, diffusion tensor imaging (DTI) measures have demonstrated reduced fractional anisotropy (FA) in the CST (3–5).

The central assumption is that FA reflects white matter integrity, as intact axonal and myelin boundaries will restrict diffusion perpendicular to the white matter fibres and thus increase FA, while loss of white matter integrity will reduce diffusion restriction and thus lower FA (6). However, besides white matter integrity, DTI measures are influenced by

multiple other factors such as crossing fibres, fibre reorganization, increased membrane permeability, destruction of intracellular compartments, and glial alterations (6,7). Which of these factors are the leading causes of reduced FA in the CST in ALS, might be elucidated by application of additional magnetic resonance imaging (MRI) contrasts.

Other MRI contrasts that might increase our insight into the degenerative changes within the CST in patients with ALS include quantitative  $T_1$  mapping ( $qT_1$  mapping), magnetization transfer contrast (MTC; expressed using the magnetization transfer ratio, MTR) and chemical exchange saturation transfer (CEST). It has been shown that the image intensities found in  $qT_1$  mapping can be used as a marker for the degree of myelination in disease and during brain development (8–10). MTR reflects the exchange between water bound to macromolecules

\*These authors contributed equally to the manuscript.

Correspondence: J. Hoogduin, University Medical Centre Utrecht, Department of Radiology (HP E01.132), P.O. Box 85500, 3508 GA, Utrecht, The Netherlands. Fax: + 31-30-2581098. E-mail: j.m.hoogduin-2@umcutrecht.nl

(Received 21 June 2013; accepted 9 September 2013)

ISSN 2167-8421 print/ISSN 2167-9223 online © 2014 Informa Healthcare  
DOI: 10.3109/21678421.2013.844168

and the unbound water fraction. Correlations of MTR with neuronal integrity or the degree of myelination have been shown (11). For example, patients with multiple sclerosis have been reported to show a global decrease in MTR (12). CEST is a relatively new imaging modality, a particular type of magnetization transfer experiment focused on measuring exchange of protons between specific solutes and free water. CEST can be used to study endogenous exchanging protons, such as amide protons resonating at +3.5 ppm from water, resulting in amide proton transfer weighted imaging, APTw imaging (13). Amide protons are abundantly present in protein backbones and peptides, and APTw imaging is expected to reflect physiological changes in this specific proton pool in case of disease. It has been suggested that APTw imaging may be sensitive for myelination (13,14), and it would be of interest to see if APT measurements can contribute to the further understanding of ALS pathology.

In this study we investigated whether measures of  $qT_1$ , MTR and APTw imaging, applied at ultra-high field (7 Tesla), might help to disentangle which factors contribute to the FA reduction in the CST of patients with ALS and provide more detailed in vivo tissue characterization.

## Material and methods

### Subjects

Eleven patients with ALS (mean age 55.5 years; range 35–71 years; eight males and three females) and nine age- and gender-matched healthy controls (mean age 54.2 years; range 36–67 years; seven males and two females) were included in this study. Patients, diagnosed according to the El Escorial criteria, were recruited from the ALS outpatient clinic of the University Medical Centre Utrecht, excluding subjects with a history of brain injury,

epilepsy, psychiatric illness and other neurodegenerative diseases. Demographic and clinical characteristics are provided in Table I, including the functional impairment as measured using the ALSFRS-R. The local Medical Ethics Committee for Research in Humans approved the study and written informed consent was obtained from all subjects, in concordance with the Declaration of Helsinki.

### MRI hardware

DTI data were acquired on a 3 T whole body MR scanner (Philips Medical Systems, Best, The Netherlands). The body coil and eight-channel head coil (Nova Medical Inc., Burlington, MA, USA) were used for signal transmission and reception, respectively.

Quantitative  $T_1$ , MTR, and APTw imaging measurements were performed at a 7T whole body MR scanner (Philips Medical Systems, Cleveland, USA). A quadrature birdcage transmit head coil (Nova Medical Inc., Burlington, MA, USA) was used in combination with a receive-only coil (Nova Medical Inc., Burlington, MA, USA). A  $B_0$  mapping sequence was included, covering the brain volume. This was then used to optimize the shim settings up to the third order.

### DTI and fibre tracking

DTI measurements were acquired using methods described earlier (5,15). Calculation of the DTI parameters was performed using the ExploreDTI toolbox (16). After brain extraction, DTI volumes were corrected for residual eddy current and motion artifacts by aligning the diffusion weighted images to the  $b = 0$  s/m<sup>2</sup> image using 3D affine registration and reorientation of the B-matrix (17). Tensor values were estimated using the RESTORE algorithm (18).

Table I. Demographic and clinical characteristics of the patients.

	Gender	Age (years)	Site of onset	Time to diagnosis (months)	Disease duration (months)	EE	ALSFRS-R	PR	B score	UL score	LL score
1	F	65	LL	11	15	prob	39	0.6	11	6	3
2	M	51	LL	22	33	prob	41	0.2	12	8	3
3	M	47	UL	2	16	poss	40	0.5	11	3	7
4	M	35	UL	9	45	prob	31	0.4	11	3	2
5	M	39	UL	2	42	poss	38	0.2	12	3	6
6	M	58	LL	11	25	prob-LS	44	0.2	12	8	5
7	M	63	LL	12	25	prob	42	0.2	12	7	3
8	F	61	UL	12	18	def	38	0.6	9	5	7
9	F	60	UL	11	21	prob	46	0.1	12	6	8
10	M	61	UL	10	15	prob	40	0.5	12	6	5
11	M	71	UL	3	17	prob-LS	31	1.0	12	2	4
		55.5 (11.2)		9.5 (5.8)	24.7 (10.8)		39.1 (4.7)	0.4 (0.3)			

F: female; M: male; B: bulbar; UL: upper limbs; LL: lower limbs; EE: El Escorial category; poss: possible; prob-LS: probable laboratory supported; prob: probable; def: definite; ALSFRS-R: revised ALS functional rating scale; PR: progression rate (48 – ALSFRS-R/disease duration).

At the bottom row of the table mean values and standard deviations (between brackets) are provided.

Finally, DTI based parameter volumes were transformed to MNI-space. We further investigated the effects in FA by looking at the changes in longitudinal diffusivity ( $D_{\text{long}}$ ) and transversal diffusivity ( $D_{\text{trans}}$ ).

Fibre streamlines were selected by placing seed regions of interest (ROIs) in both the left or right motor tract at the level of the pons. Fibre tracking was then performed by deterministic streamline fibre tractography (19) from 125 seed points distributed homogeneously over each voxel in the seed ROI. The following settings for streamline reconstruction were applied: minimal FA = 0.2, maximal angle =  $20^\circ$ , streamline step size = 1 mm, minimal/maximal fibre length = 40/500 mm. Additional selection criteria were placed as an inclusion ROI at the level of the primary motor cortex to select those streamlines that connected both the pons level and cortical level ROIs. Two exclusion ROIs were placed to prevent inter-hemispheric crossover and connections to the cerebellum (Figure 1).

### $T_1$ mapping

A multi-slice  $T_1$  mapping sequence was acquired (20–22). In this  $T_1$  mapping approach, after an inversion pulse, all slices in the volume are acquired successively using slice-selective  $90^\circ$  excitations and EPI readouts. During the following repetitions, the slice ordering is shifted, so all slices are acquired at different inversion times. A slice-shift of two slices was applied, so that in 23 repetitions, all 46 slices were sampled at 23 different time-points after inversion, allowing for robust and precise estimation of the longitudinal relaxation time. Details on the acquisition

sequence are provided in the supplementary data – please find this material with the following direct link to the article: <http://informahealthcare.com/doi/abs/10.3109/21678421.2013.844168>.

The longitudinal relaxation time  $T_1$  is a central MR parameter that reflects the capability of the spin-lattice to relax longitudinal magnetization back to equilibrium. In normal tissue, the speed of relaxation is directly dependent on the amount and nature of interactions of the bulk water with the surrounding lattice. In free water such as CSF (around 4500 ms at 7T),  $T_1$  is long, and in structured tissue such as myelinated white matter,  $T_1$  is short (around 1100 ms at 7T). By quantitatively determining the longitudinal relaxation time, as opposed to weighting an image with an unknown amount of  $T_1$  effect, we can discriminate small changes in  $T_1$ , and thus identify small changes due to pathology (23).

### MTR and APTw imaging

MTR and APTw imaging were conducted using the pulsed steady state method as previously described (24).

**Magnetization transfer ratio (MTR).** Magnetization transfer imaging is a technique that probes the macromolecular environment of bulk water protons by assessing the amount of magnetization transfer from the bound water to the bulk water pool. This is done in a saturation transfer experiment, where the amount of signal reduction directly reflects the amount of bound water molecules

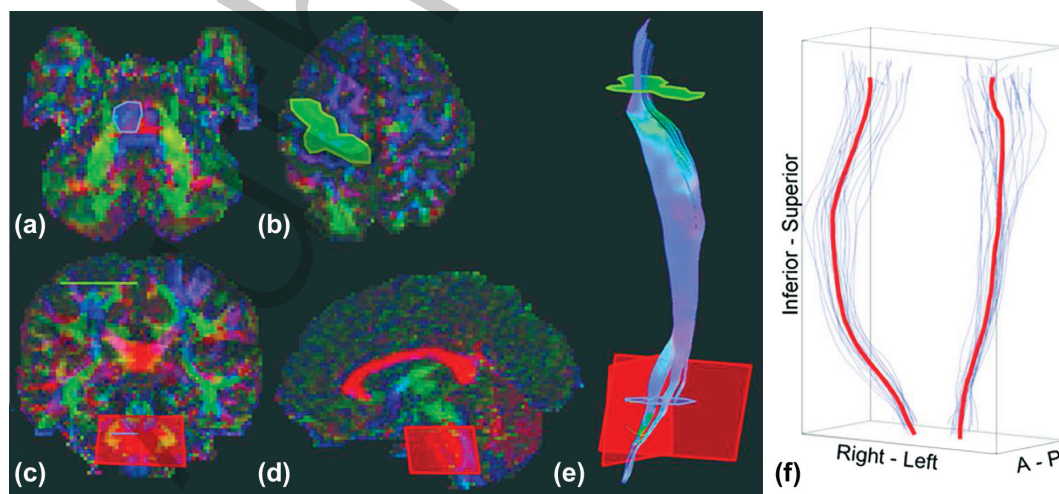


Figure 1. CST selection procedure. This figure shows the location of the regions of interest (ROIs) for the selection of the CST fibre bundles. (a) At the level of the pons a seed region (blue encircled) was placed on an axial slice, the fibre direction was indicated by colour. From this ROI the fibre tracking was initiated. (b) Another ROI (green) was placed directly on the primary motor cortex (precentral gyrus) selecting all fibres both crossing the pons and the motor cortex. (c) To exclude fibres connecting the cerebellum, an ROI (red) was placed in the coronal plane, deselecting all fibres crossing this ROI. (d) A second, excluding ROI (red) was placed in the sagittal plane to deselect fibres connecting the other hemisphere. (e) This procedure resulted in a number of fibres, together forming a reconstruction of the CST. (f) For each subject an average fibre curve (blue) was calculated, resulting in two group-average curves for the left and right CST (red).

(and therefore macromolecular content). To compare the amount of magnetization transfer between subjects, the saturation effect is expressed in the MTR, which quantifies the amount of signal suppression due to magnetization transfer. The amount of magnetization transfer contrast is directly dependent on the amount of myelination of the tissue, with areas that are strongly myelinated showing large MTR values such as the corpus callosum, while deep white matter, subcortical white matter u-fibres and grey matter areas display decreasing MTR values (25).

Because the off-resonance frequency is relatively close to the water resonance, it is expected that direct water saturation has a significant effect on the total observed saturation. To correct for this, we fit and remove a Lorentzian lineshape from the measured saturation curves as described in the supplementary data – please find this material with the following direct link to the article: <http://informahealthcare.com/doi/abs/10.3109/21678421.2013.844168>.

*Amide proton transfer weighted (APT<sub>w</sub>) imaging.* Another, more specific, mechanism for measuring magnetization exchange is by sensitizing for chemical exchange using a method called CEST. This method has gained much attention in the last few years, because it offers a fundamental insight into the chemical nature of the tissue, probing the concentration and exchange rates of endogenous amide protons (26). CEST measurements are performed by repeating MT measurement with varying off-set frequencies of the saturation pulse. This results in a sampling of the Z-spectra, which is roughly symmetric around the water resonance, except for those frequencies where the exchanging protons resonate. By means of asymmetry analysis, i.e. taking the difference between saturated image at the resonance frequency of interest and its opposite counterpart frequency, chemical transfer effects can be distinguished from the conventional MT effects. In this work, we focus on the exchanging amide protons, which resonate at +3.5 ppm from the water resonance, and the resulting images are called APT<sub>w</sub> images. For many applications amide protons are of interest, due to their increased natural abundance in pathology and appropriate exchange rates for saturation experiments (27,28).

#### *Quantitative comparison*

For quantitative comparison, qT<sub>1</sub>, MTR, and APT<sub>w</sub> volumes were registered to each subject's FA map by rigid body registration using a normalized mutual information cost function and tri-linear interpolation. For the MTR based volumes, the 4.03-ppm saturated image was used in the registration procedure and the resulting transformation matrix was used for all following parameter maps.

Averaged normalized histograms were compared to evaluate the MR contrasts between patients and controls at a whole brain level. The histograms were calculated over all voxels in the brain volume, excluding those that were obviously affected by signal voids due to air-tissue boundaries, such as near the nasal cavities and ear-canals, as observed in EPI based methods. Included in these histograms were grey matter and the ventricles, so a contribution of cerebrospinal fluid (CSF) is to be expected. After normalizing to their total count, the average histograms for patients and controls were calculated and plotted with the accompanying standard deviations.

The goal of the tract-based analysis was to compare quantitative MRI measures along the CST, while allowing for inter-subject variation of each 3D trajectory. Following the method described in (29), each subject's reconstructed CST (consisting of a collection of ~150 streamline trajectories) was averaged to a single curve. The values of the different MRI contrasts of interest of the voxels crossed by the fibre trajectories were mapped to the nearest corresponding point on the curve. As a result, each subject's curve reflects the averaged values along that curve. Similarly, the group average curves were calculated by taking the average curve over all subjects. The resulting two averaged curves correspond to the group-average left and right CST. We report the median values ( $\pm$  interquartile ranges) for each MR contrast (FA, D<sub>long</sub>, D<sub>trans</sub>, qT<sub>1</sub>, MT, and APT<sub>w</sub>) along the CST.

#### *Statistical analysis*

The entire brain volumes were compared between patients and controls by testing for difference between the mean values for each subject, using a two-tailed *t*-test. The multiple measures along the left and right CST sections were compared, for each modality, between patients and controls using a repeated measurements analysis by a linear mixed-effects model with maximum likelihood estimation (ML), including group assignment (patient or healthy control) as a factor and gender as a covariate. Additionally, for each separate point along the group-averaged tract, the measures in patients and controls were compared using a Mann-Whitney, Wilcoxon or rank test. The effect size was calculated by calculating the difference between the medians. For all analyses, a statistical threshold of  $p \leq 0.05$  was considered statistically significant.

## **Results**

### *Whole brain histogram analysis*

At the whole brain level, based on histogram analysis, none of the MR contrasts revealed any significant differences between patients and controls. Figure 2 shows the whole brain histograms for each

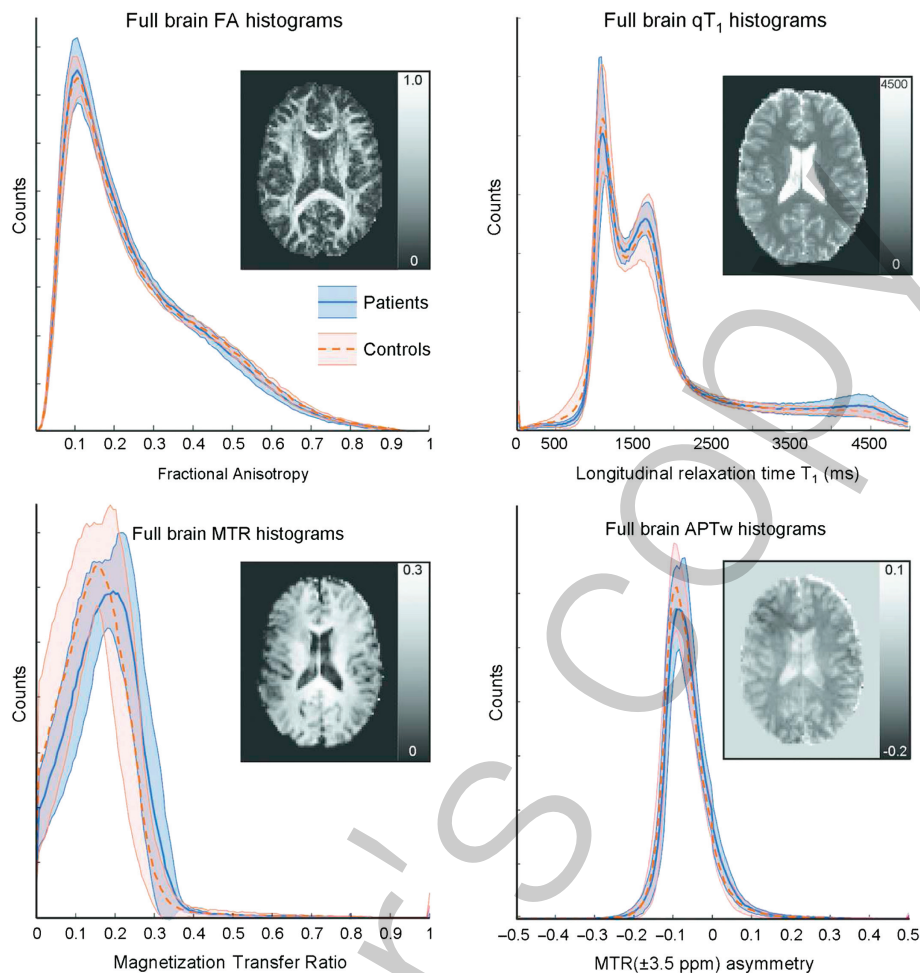


Figure 2. Average whole brain histograms for FA,  $qT_1$ , MTR, and APTw imaging. Blue and pink indicate the mean with standard deviations for patients and controls, respectively. Each histogram includes an example slice of a single subject. No significant differences were found in these whole brain analyses.

MR contrast, with an example slice of a single subject. A difference in the MTR peak locations for patients (0.19) and controls (0.15) can be observed. However, the whole brain average MT values did not show significant differences between patients and controls.

#### Corticospinal tract measures

We report the values of several MR contrasts measured along the fibre tractography streamlines of the CST. Because the coverage of the DTI volume is larger than that of the other contrasts, we focus here on the region of the CST where all acquired volumes overlapped. In the presented results, we show the median values over the left and right group averaged CST each consisting of 41 points, spanning roughly 8 cm in the feet-head direction.

The tract specific measures along the CST revealed a significantly reduced FA in patients compared to controls along the right CST ( $p = 0.01$ ) and a trend-like reduced FA along the left CST ( $p = 0.09$ ). Figure 3a shows the FA measures for patients and controls along the tract, and significantly reduced FA was found both in the subcortical region (right

and more caudally (posterior limb of the internal capsule, left and right). Diffusivity transverse to the largest direction of diffusion,  $D_{\text{trans}}$  shows a significant increase along the right CST ( $p = 0.04$ ). The measures over the left CST are not significantly different in patients compared to controls ( $p = 0.15$ ), similar to the FA results (Figure 3b). Longitudinal diffusivity,  $D_{\text{long}}$  measures are not significantly different along the CST (left  $p = 0.37$ ; right  $p = 0.46$ ), indicating that the change in FA originates from an increased  $D_{\text{trans}}$  in the patient group (Figure 3c).

No significant changes in  $qT_1$  (Figure 3d) values were found (left  $p = 0.58$ ; right  $p = 0.34$ ). The MTR measures (Figure 3e) demonstrated a significant increase in patients compared to controls along the right CST ( $p = 0.05$ ), and again the changes in the left CST were not significant ( $p = 0.24$ ). APTw scores along the averaged fibre bundles showed no significant changes between patients and controls (left  $p = 0.50$ ; right  $p = 0.21$ ) (Figure 3f). In a post hoc analysis we examined the correlation between MTR and both  $D_{\text{trans}}$  and FA. In Supplementary Figure 1 – please find this material with the following direct link to the article: <http://informahealthcare.com/doi/abs/10.3109/21678421.2013.844168>,

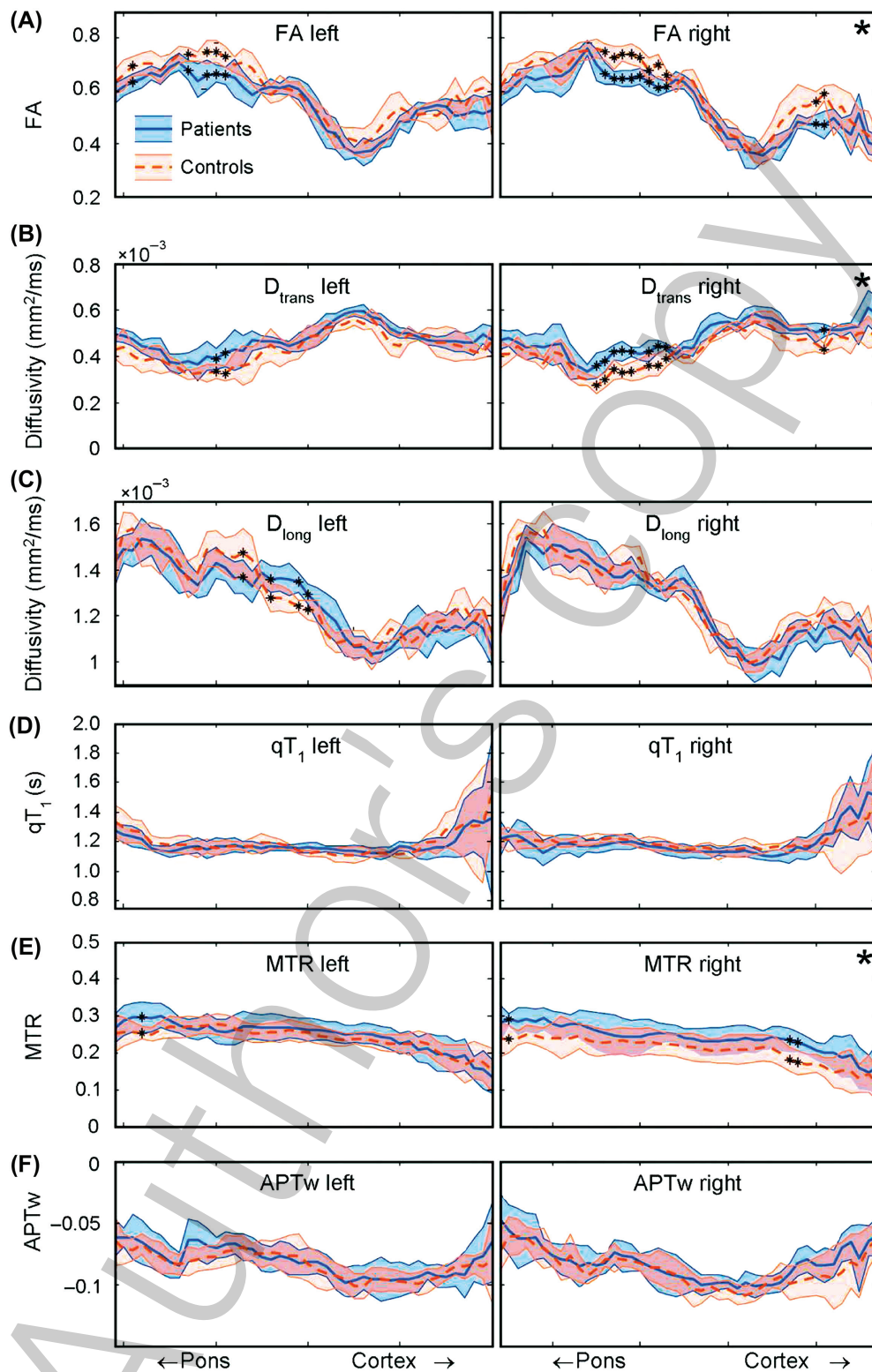


Figure 3. Quantitative MR measures along the CST. MR measures along the tract were sampled every 2 mm and the group results for patients (blue) and controls (red) were plotted for the left and right motor tracts. The median values and interquartile ranges are shown. Measurements along the tract highlighted with \* showed significant differences (Mann-Whitney, Wilcoxon test,  $p < 0.05$ , two-tailed). The plots marked with a \* in the upper right corner showed significant differences over the complete CST section. (a) FA values were significantly lower in patients compared to controls along the right CST; however, also the left CST shows a subtrajectory with significantly reduced FA measures. (b)  $D_{\text{trans}}$  showed significantly increased in patients compared to controls along the right CST similar to the changes in FA. (c)  $D_{\text{long}}$  showed no consistent differences between patients and controls. (d)  $qT_1$  showed no significant differences between patients and controls. The measures in the cortical grey matter (right side of the plot) showed more variation compared to the white matter trajectory as was expected. (e) MTR showed a significant increase along the right CST in patients compared to controls. (f) APTw imaging showed no significant changes between patients and controls.

for personal use only, do not copy

the significantly negative relation between MTR and  $D_{\text{trans}}$  ( $p = 1.2 \cdot 10^{-4}$ ) and the positive relation between MTR and FA ( $p = 4.8 \cdot 10^{-11}$ ) is shown. It is important to note, however, that these measures are not completely independent (repeated measurements within the same subject) and therefore the level of significance might be overestimated. We additionally performed a regression analysis using a linear mixed-effects model correcting for repeated measurements within the same subject; this resulted in a significant relation as well ( $p < 0.05$ ).

We did not find a significant correlation using Pearson's correlation testing between imaging measures (averaged along the CST) and clinical markers (ALSFRS-R, progression rate (48 – ALSFRS-R/disease duration) and disease duration).

## Discussion

In this study, quantitative MR parameters were compared between ALS patients and age-matched healthy controls, both in a 'whole brain' analysis, as well as specifically along the CST. We found a significant decrease in FA along the right CST, consistent with previous studies (3,5,30). Increased diffusivity perpendicular to the CST ( $D_{\text{trans}}$ ) was found underlying the decrease in FA. Additionally, exploratory data, acquired on ultra-high field MRI, showed a significant increase in MTR in the right CST in the patient group. The other MRI contrasts,  $qT_1$  and APTw imaging, did not reveal significant changes.

We observed a reduced FA both subcortical and in the posterior limb of the capsula interna, which is consistent with previous findings (5,30). To gain more insight into the underlying changes in the brain tissue causing reduced FA in the CST, other diffusion-based parameters were assessed. Decomposing the FA values into the longitudinal and transverse diffusivities (parallel and perpendicular) to the CST direction revealed a significantly increased  $D_{\text{trans}}$  and no significant changes in  $D_{\text{long}}$  in patients compared to controls. An increase in the observed  $D_{\text{trans}}$  indicates a loss of diffusion restriction perpendicular to the main direction of diffusion. Diffusivity changes were asymmetrical with predominant changes within the right CST, which has been repeatedly observed in ALS (31–33). It has been suggested that the right hemisphere is more vulnerable to the neurodegenerative process (34).

MTR is considered an indicator for the capacity of water bound to macromolecules in (nervous) tissue to exchange magnetization with unbound water molecules (14). In white matter tissue, MTR is mainly determined by the myelin content and, to a lesser extent, the number of axons or gliosis (35). Demyelination has been demonstrated to cause a reduced MTR; however, in this study we found a significant increase of MTR in the right CST. This

finding is different from what we expected and from what has been previously reported (36,37); therefore we need to interpret these data cautiously. However, since MTR is sensitive for the magnetization transfer between macromolecular and liquid protons, an increase of the liquid fraction in tissue has the potential to increase MTR (11). This hypothesis is supported by the finding of increased transverse diffusion, which might also be caused by an increased liquid fraction. Another potential cause of increased MTR in ALS might be the accumulation of pathological protein aggregates (macromolecules) – as is well known to occur in ALS. The correspondence of predominant changes in the right CST for diffusivity characteristics and MTR measures increases the credibility of our findings. The combination of decreased FA and increased MTR in the CST of patients is remarkable since in general a decreased FA (e.g. due to demyelination) is related to a decreased MTR. Therefore, we further assessed the relationship between FA and MTR – in a post hoc analysis – by assessing the correlation between these two parameters within individual subjects. This analysis confirmed a positive correlation between these two modalities, indicating that at a group level it is unlikely that demyelination is the primary cause of reduced FA in patients. In summary, an increased tissue liquid fraction, potentially in combination with protein accumulation, might have caused an overall increase of MTR values in patients (38). These effects apparently outweigh some degree of demyelination, which is supported by findings in post mortem studies in ALS (39,40). Based on these data, pathological changes which lead to an increase in the liquid fraction such as proliferation of glial cells and extracellular matrix expansion (41–43) are more likely to be the primary cause of reduced FA within the CST of patients with ALS.

CEST and quantitative  $T_1$  imaging measurements did not show significant differences between patients and controls along the CST. APTw imaging – a variant of CEST – at high field has been suggested as a non-invasive biomarker of white matter pathology, potentially providing complementary information to other MRI methods in current clinical use (26). Grey matter is known to show lower APTw contrast compared to white matter, potentially due to fewer membrane-associated (extracellular, cytosolic, and transmembrane) proteins such as those found in myelin (13). However, for ALS, APTw imaging has not shown the same sensitivity for white matter pathology as FA. More research on the effects of brain tissue pathology and the APTw contrasts is needed to further elucidate its dynamics in health and disease. No changes in  $T_1$  contrast were found, which is in contrast to previously published results showing that  $T_1$  weighted imaging with MTC enhancement allowed for the visualization of CST lesions (44,45).  $T_1$  contrast has also been shown to be related to the degree of



myelination and the amount of bulk water (46). For example, lesions in MS showed shortened  $T_1$  values indicating plaque formation while global histogram analysis indicated elongated  $T_1$  values, suggesting diffuse demyelination (47,48). To rule out effects in  $qT_1$  that might have been missed in the tract specific analysis due to misregistration of the  $qT_1$  parameter maps to their corresponding FA volumes, the whole brain volumes were compared using a post hoc VBM analysis to highlight significant differences (data not shown). This additional analysis did not yield any significant results. Together with our results in MTR, the lack of effects in APTw and  $qT_1$  imaging might lend further support that demyelination is not the main cause of FA decrease found in the CST of ALS patients (42,43).

Given the exploratory nature of this study, there are limitations with which these results need to be interpreted. First, the sample size of patients and controls employed in this study is small and the variation of the measurements between subjects is relatively large, hampering the detection of subtle differences. Secondly, the modelling of MTR based methods, especially the calculation of APTw images is still a very active field of research, and it is expected that future developments will improve both the sensitivity and reproducibility of this new method and that more factors influencing or contributing to this MR contrast will be elucidated.

To conclude, we explored multiple MR contrasts at ultra-high field in relation to FA reduction in the CST of patients with ALS. MR contrasts were selected based on their sensitivity to neuronal loss and/or demyelination of white matter. A reduced FA in the CST of patients with ALS was confirmed, and further was shown to originate from an increase in  $D_{\text{trans}}$ . In addition, we found an increase in MTR in the right CST, which together with the diffusivity findings completes the white matter profile in ALS. This profile is inconsistent with demyelination as cause of reduced FA but consistent with an increase of free liquid spins, pointing in the direction of tissue changes such as proliferation of glial cells and extracellular matrix expansion. Future studies are needed to validate our findings in larger groups of patients and further advances in both MR technology and neuroscience are needed to increase insights into the dynamics of these MR contrasts in health and disease.

### Acknowledgements

The authors are grateful for the time and effort which patients, their caregivers and healthy controls invested in this study.

**Declaration of interest:** LvdB served on the Advisory Boards of Biogen and Cytokinetics, and received a travel grant and speaker fees from Baxter.

The authors alone are responsible for the content and writing of the paper.

### References

1. Smith MC. Nerve Fibre Degeneration in the Brain in Amyotrophic Lateral Sclerosis. *J Neurol Neurosurg Psychiatry*. 1960;23:269–82.
2. Turner MR, Agosta F, Bede P, Govind V, Lule D, Verstraete E. Neuroimaging in amyotrophic lateral sclerosis. *Biomark Med*. 2012;6:319–37.
3. Filippini N, Douaud G, Mackay CE, Knight S, Talbot K, Turner MR. Corpus callosum involvement is a consistent feature of amyotrophic lateral sclerosis. *Neurology*. 2010; 75:1645–52.
4. Agosta F, Pagani E, Petrolini M, Caputo D, Perini M, Prellè A, et al. Assessment of white matter tract damage in patients with amyotrophic lateral sclerosis: a diffusion tensor MR imaging tractography study. *AJNR Am J Neuroradiol*. 2010;31:1457–61.
5. Verstraete E, van den Heuvel MP, Veldink JH, Blanken N, Mandl RC, Hulshoff Pol HE, et al. Motor network degeneration in amyotrophic lateral sclerosis: a structural and functional connectivity study. *PLoS One*. 2010;5: e13664.
6. Beaulieu C. The basis of anisotropic water diffusion in the nervous system: a technical review. *NMR in Biomedicine*. 2002;15:435–55.
7. Acosta-Cabronero J, Williams GB, Pengas G, Nestor PJ. Absolute diffusivities define the landscape of white matter degeneration in Alzheimer's disease. *Brain*. 2010;133: 529–39.
8. Glasser MF, van Essen DC. Mapping human cortical areas in vivo based on myelin content as revealed by T1- and T2-weighted MRI. *J Neurosci*. 2011;31:11597–616.
9. Paus T, Collins DL, Evans AC, Leonard G, Pike B, Zijdenbos A. Maturation of white matter in the human brain: a review of magnetic resonance studies. *Brain Res Bull*. 2001;54: 255–66.
10. Barkovich AJ. Magnetic resonance techniques in the assessment of myelin and myelination. *J Inherit Metab Dis*. 2005;28:311–43.
11. Henkelman RM, Stanisz GJ, Graham SJ. Magnetization transfer in MRI: a review. *NMR Biomed*. 2001;14:57–64.
12. Moll NM, Rietsch AM, Thomas S, Ransohoff AJ, Lee JC, Fox R, et al. Multiple sclerosis normal-appearing white matter: pathology-imaging correlations. *Ann Neurol*. 2011; 70:764–73.
13. Dula AN, Asche EM, Landman BA, Welch EB, Pawate S, Sriram S, et al. Development of chemical exchange saturation transfer at 7T. *Magn Reson Med*. 2011;66:831–8.
14. Mougou OE, Coxon RC, Pitiot A, Gowland PA. Magnetization transfer phenomenon in the human brain at 7T. *Neuroimage*. 2010;49:272–81.
15. Verstraete E, Veldink JH, Mandl RC, van den Berg LH, van den Heuvel MP. Impaired structural motor connectome in amyotrophic lateral sclerosis. *PLoS One*. 2011;6: e24239.
16. Polders DL, Leemans A, Hendrikse J, Donahue MJ, Luijten PR, Hoogduin JM. Signal to noise ratio and uncertainty in diffusion tensor imaging at 1.5, 3.0, and 7.0 Tesla. *J Magn Reson Imaging*. 2011;33:1456–63.
17. Leemans A, Jones DK. The B-matrix must be rotated when correcting for subject motion in DTI data. *Magn Reson Med*. 2009;61:1336–49.
18. Chang LC, Jones DK, Pierpaoli C. RESTORE: robust estimation of tensors by outlier rejection. *Magn Reson Med*. 2005;53:1088–95.
19. Basser PJ, Pajevic S, Pierpaoli C, Duda J, Aldroubi A. In vivo fibre tractography using DT-MRI data. *Magn Reson Med*. 2000;44:625–32.

20. Ordidge RJ, Gibbs P, Chapman B, Stehling MK, Mansfield P. High-speed multislice T1 mapping using inversion-recovery echo-planar imaging. *Magn Reson Med.* 1990; 16:238–45.
21. Clare S, Jezzard P. Rapid T(1) mapping using multislice echo planar imaging. *Magn Reson Med.* 2001;45:630–4.
22. Polders DL, Leemans A, Luijten PR, Hoogduin H. Uncertainty estimations for quantitative in vivo MRI T1 mapping. *J Magn Reson.* 2012;224:53–60.
23. Deoni SC. Quantitative relaxometry of the brain. *Top Magn Reson Imaging.* 2010;21:101–13.
24. Jones CK, Polders D, Hua J, Zhu H, Hoogduin HJ, Zhou J, et al. In vivo three-dimensional whole-brain pulsed steady-state chemical exchange saturation transfer at 7T. *Magn Reson Med.* 2012;67:1579–89.
25. Tofts PS, Steens CA, van Buchem MA. Quantitative MRI of the Brain: Measuring Changes Caused by Disease. 2003;258–98.
26. van Zijl PC, Yadav NN. Chemical exchange saturation transfer (CEST): what is in a name and what isn't? *Magn Reson Med.* 2011;65:927–48.
27. Zhou J, Payen JF, Wilson DA, Traystman RJ, van Zijl PC. Using the amide proton signals of intracellular proteins and peptides to detect pH effects in MRI. *Nat Med.* 2003; 9:1085–90.
28. Polders DL, Hoogduin JM. Chemical Exchange Saturation Transfer MR Imaging: Potential Clinical Applications. *PET Clinics.* 2013; in press.
29. Mandl RC, Schnack HG, Luijckx J, van den Heuvel MP, Cahn W, Kahn RS, et al. Tract-based Analysis of Magnetization Transfer Ratio and Diffusion Tensor Imaging of the Frontal and Frontotemporal Connections in Schizophrenia. *Schizophr Bull.* 2010;36:778–87.
30. van der Graaff MM, Sage CA, Caan MW, Akkerman EM, Lavini C, Majoie CB, et al. Upper and extramotor neuron involvement in early motor neuron disease: a diffusion tensor imaging study. *Brain.* 2011;134:1211–28.
31. Cosottini M, Pesaresi I, Piazza S, Diciotti S, Cecchi P, Fabbri S, et al. Structural and functional evaluation of cortical motor areas in amyotrophic lateral sclerosis. *Exp Neurol.* 2012;234:169–80.
32. Agosta F, Pagani E, Rocca MA, Caputo D, Perini M, Salvi F, et al. Voxel-based morphometry study of brain volumetry and diffusivity in amyotrophic lateral sclerosis patients with mild disability. *Hum Brain Mapp.* 2007; 28:1430–8.
33. Kassubek J, Unrath A, Huppertz HJ, Lule D, Ethofer T, Sperfeld AD, et al. Global brain atrophy and corticospinal tract alterations in ALS, as investigated by voxel-based morphometry of 3-D MRI. *Amyotroph Lateral Scler.* 2005; 6:213–20.
34. Chen Z, Ma L. Grey matter volume changes over the whole brain in amyotrophic lateral sclerosis: a voxel-wise meta-analysis of voxel based morphometry studies. *Amyotroph Lateral Scler.* 2010;11:549–54.
35. Stanisz GJ, Kecojevic A, Bronskill MJ, Henkelman RM. Characterizing white matter with magnetization transfer and T(2). *Magn Reson Med.* 1999;42:1128–36.
36. Kato Y, Matsumura K, Kinosada Y, Narita Y, Kuzuhara S, Nakagawa T. Detection of pyramidal tract lesions in amyotrophic lateral sclerosis with magnetization-transfer measurements. *AJNR Am J Neuroradiol.* 1997;18:1541–7.
37. Tanabe JL, Vermathen M, Miller R, Gelinus D, Weiner MW, Rooney WD. Reduced MTR in the corticospinal tract and normal T2 in amyotrophic lateral sclerosis. *Magn Reson Imaging.* 1998;16:1163–9.
38. da Rocha AJ, Maia AC Jr, Valerio BC. Corticospinal tract MR signal-intensity pseudonormalization on magnetization transfer contrast imaging: a potential pitfall in the interpretation of the advanced compromise of upper motor neurons in amyotrophic lateral sclerosis. *AJNR Am J Neuroradiol.* 2012;33:79–80.
39. Iwanaga K, Hayashi S, Oyake M, Horikawa Y, Hayashi T, Wakabayashi M, et al. Neuropathology of sporadic amyotrophic lateral sclerosis of long duration. *J Neurol Sci.* 1997;146:139–43.
40. Ikeda K, Akiyama H, Arai T, Ueno H, Tsuchiya K, Kosaka K. Morphometrical reappraisal of motor neuron system of Pick's disease and amyotrophic lateral sclerosis with dementia. *Acta Neuropathol.* 2002;104:21–8.
41. Hughes JT. Pathology of amyotrophic lateral sclerosis. *Adv Neurol.* 1982;36:61–74.
42. Phillips T, Robberecht W. Neuroinflammation in amyotrophic lateral sclerosis: role of glial activation in motor neuron disease. *Lancet Neurol.* 2011;10:253–63.
43. Ince PG, Highley JR, Kirby J, Wharton SB, Takahashi H, Strong MJ, et al. Molecular pathology and genetic advances in amyotrophic lateral sclerosis: an emerging molecular pathway and the significance of glial pathology. *Acta Neuropathol.* 2011;122:657–71.
44. da Rocha AJ, Oliveira AS, Fonseca RB, Maia AC Jr, Buainain RP, Lederman HM. Detection of corticospinal tract compromise in amyotrophic lateral sclerosis with brain MR imaging: relevance of the T1-weighted spin-echo magnetization transfer contrast sequence. *AJNR Am J Neuroradiol.* 2004;25:1509–15.
45. Carrara G, Carapelli C, Venturi F, Ferraris MM, Lequio L, Chio A, et al. A distinct MR imaging phenotype in amyotrophic lateral sclerosis: correlation between T1 magnetization transfer contrast hyperintensity along the corticospinal tract and diffusion tensor imaging analysis. *AJNR Am J Neuroradiol.* 2012;33:733–9.
46. Fatouros PP, Marmarou A. Use of magnetic resonance imaging for in vivo measurements of water content in human brain: method and normal values. *J Neurosurg.* 1999;90: 109–15.
47. Neema M, Stankiewicz J, Arora A, Dandamudi VS, Batt CE, Guss ZD, et al. T1- and T2-based MRI measures of diffuse grey matter and white matter damage in patients with multiple sclerosis. *J Neuroimaging.* 2007;17 (Suppl 1): S16–21.
48. Vrenken H, Geurts JJ, Knol DL, van Dijk LN, Dattola V, Jaspers B, et al. Whole-brain T1 mapping in multiple sclerosis: global changes of normal-appearing grey and white matter. *Radiology.* 2006;240:811–20.

**Supplementary material available online**

Supplementary Figure 1.